



Communication: Equilibrium rate coefficients from atomistic simulations: The $O(3P) + NO(2\Pi) \rightarrow O_2(X\ 3\Sigma\ g^-) + N(4S)$ reaction at temperatures relevant to the hypersonic flight regime

Juan Carlos Castro-Palacio, Raymond J. Bemish, and Markus Meuwly

Citation: *The Journal of Chemical Physics* **142**, 091104 (2015); doi: 10.1063/1.4913975

View online: <http://dx.doi.org/10.1063/1.4913975>

View Table of Contents: <http://scitation.aip.org/content/aip/journal/jcp/142/9?ver=pdfcov>

Published by the AIP Publishing

Articles you may be interested in

[Exploring mechanisms of a tropospheric archetype: \$CH_3O_2 + NO\$](#)

J. Chem. Phys. **143**, 234302 (2015); 10.1063/1.4937381

[Communication: Spectroscopic consequences of proton delocalization in \$OCHCO^+\$](#)

J. Chem. Phys. **143**, 071102 (2015); 10.1063/1.4929345

[Selected-ion flow tube temperature-dependent measurements for the reactions of \$O_2^+\$ with N atoms and \$N_2^+\$ with O atoms](#)

J. Chem. Phys. **142**, 154305 (2015); 10.1063/1.4916913

[Computational study of collisions between \$O\(3P\)\$ and \$NO\(2\Pi\)\$ at temperatures relevant to the hypersonic flight regime](#)

J. Chem. Phys. **141**, 164319 (2014); 10.1063/1.4897263

[Simulation of hypersonic flows using a detailed nitric oxide formation model](#)

Phys. Fluids **9**, 1171 (1997); 10.1063/1.869205



NEW Special Topic Sections

NOW ONLINE
Lithium Niobate Properties and Applications:
Reviews of Emerging Trends

AIP Applied Physics
Reviews

Communication: Equilibrium rate coefficients from atomistic simulations: The $\text{O}(^3\text{P}) + \text{NO}(^2\Pi) \rightarrow \text{O}_2(X^3\Sigma_g^-) + \text{N}(^4\text{S})$ reaction at temperatures relevant to the hypersonic flight regime

Juan Carlos Castro-Palacio,¹ Raymond J. Bemish,² and Markus Meuwly^{1,3,a)}

¹Department of Chemistry, University of Basel, Klingelbergstrasse 80, 4056 Basel, Switzerland

²Air Force Research Laboratory, Space Vehicles Directorate, Kirtland AFB, New Mexico 87117, USA

³Department of Chemistry, Brown University, Providence, Rhode Island 02912, USA

(Received 27 January 2015; accepted 20 February 2015; published online 4 March 2015)

The $\text{O}(^3\text{P}) + \text{NO}(^2\Pi) \rightarrow \text{O}_2(X^3\Sigma_g^-) + \text{N}(^4\text{S})$ reaction is among the N- and O- involving reactions that dominate the energetics of the reactive air flow around spacecraft during hypersonic atmospheric re-entry. In this regime, the temperature in the bow shock typically ranges from 1000 to 20 000 K. The forward and reverse rate coefficients for this reaction derived directly from trajectory calculations over this range of temperature are reported in this letter. Results compare well with the established equilibrium constants for the same reaction from thermodynamic quantities derived from spectroscopy in the gas phase which paves the way for large-scale in silico investigations of equilibrium rates under extreme conditions. © 2015 AIP Publishing LLC. [<http://dx.doi.org/10.1063/1.4913975>]

Reactions involving nitrogen- and oxygen-containing small molecules occur in a wide range of processes. As an example, NO_2 —which can decay into $\text{NO} + \text{O}$ or $\text{O}_2 + \text{N}$ —plays a major role in atmospheric chemistry, as a smog constituent and in combustion processes.^{1–3} The reaction characteristics change from formation of NO_2 to exchange and dissociation reactions at higher temperatures (1000–20 000 K). Above 20 000 K, it is expected that the reactions will be dominated by the complete dissociation to the atomic species. In the hypersonic flight regime—which is the physical situation of interest in the present work—the chemistry will be in the intermediate case. Near the surface of such vehicles, highly non-equilibrium conditions will be present with vibrational and rotational temperatures independently reaching several thousand Kelvin.⁴ The gas-phase, surface reactions, and energy transfer at these temperatures are essentially uncharacterized and the experimental methodologies capable of probing them are not well established. In this respect, theoretical and validated computational approaches become a valuable complement to experiments.

In order to model chemical kinetics under such extreme and non-equilibrium conditions, state- and temperature-dependent rate coefficients for individual reactions are required. However, direct experimentation under such conditions is usually not possible. In the present work, both forward and reverse rate coefficients for $\text{O}(^3\text{P}) + \text{NO}(^2\Pi) \leftrightarrow \text{O}_2(X^3\Sigma_g^-) + \text{N}(^4\text{S})$ are calculated from molecular dynamics (MD) simulations for moderate to high temperatures (1000 to 20 000 K) and compared with results from experimentally derived thermodynamics quantities from the NASA CEA (National Aeronautics and Space Administration Chemical Equilibrium with Applications) database.^{5,6} The value of such

a validated computational approach is that it can be applied generically to a wide range of bimolecular reactions whenever direct experiments are not available, with consistency of the computations depending on a comparison of independent dynamic and energetic approaches.

A schematic representation of the relevant species for the $\text{O}(^3\text{P}) + \text{NO}(^2\Pi) \leftrightarrow \text{O}_2(X^3\Sigma_g^-) + \text{N}(^4\text{S})$ reaction is given in Figure 1. NO_2 formation has a barrier of 1.3 eV from the $\text{N} + \text{O}_2$ side, whereas from the $\text{NO} + \text{O}$ side, it is a barrierless process. In order to reach the $\text{N} + \text{O}_2$ side from the $\text{NO} + \text{O}$ side, 2.6 eV are required including the barrier. An additional 5.6 eV are required for dissociation of O_2 and 6.9 eV for the dissociation of NO to the atomization state of $\text{N} + \text{O}_2$.

Even when the excited states can approach the ground state PES for certain configurations (Figure 2), their influence can be considered to be minor. The first excited state is dissociative and about 6 eV are required to access the second and third excited states (see Figure 2). For the Maxwell-Boltzmann distribution at 20 000 K, translational energies beyond 6 eV are accessed with little probability (0.06). This provides an upper bound since a thermal distribution requires additional energy to be distributed into rotational and vibrational motion. Furthermore, lifetimes of the system at the second and third excited states are presumably small since the wells are shallow. This causes the system to rapidly return to the ground state.⁸ The expected effect of including electronically excited states is to somewhat lower the rate coefficients due to the topology of the excited PES (see Figure 2 which exhibits shallow minima that potentially stabilize intermediates for short times). Therefore, in this work, only the ground state PES is considered since it dominates the reaction dynamics under the relevant physicochemical conditions.

The equilibrium constant $K(T)$ as a function of temperature for a chemical reaction at equilibrium is

^{a)} Author to whom correspondence should be addressed. Electronic mail: m.meuwly@unibas.ch

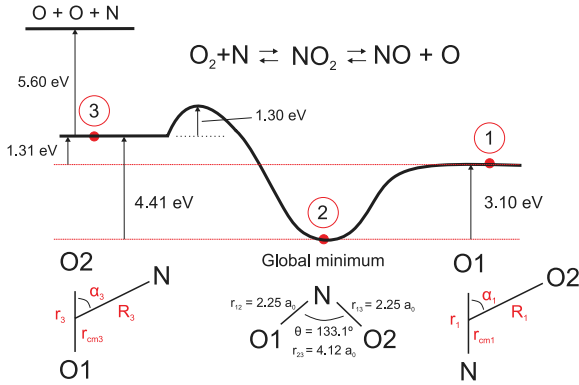


FIG. 1. Relevant stages in the NO1 + O2 reaction. The energies are those from the *ab initio* calculations in Ref. 7.

$$K(T) = \frac{k_+(T)}{k_-(T)}, \quad (1)$$

where $k_+(T)$ and $k_-(T)$ are the rate coefficients for the forward and reverse reactions, respectively. The rate coefficient for the forward reaction ($k_+(T)$) has been recently determined from atomistic simulations.⁷ The same methodology is used here for the calculation of the rate coefficient for the reverse reaction $k_-(T)$. Following the previous work, three steps are involved: (1) the construction of the PES for the ground state of the NO₂ molecule based on high-level *ab initio* calculations and its representation with a reproducing kernel Hilbert space (RKHS) method⁹ combined with Legendre polynomials; (2) quasi-classical trajectory (QCT) calculations to study the adiabatic reaction dynamics; and (3) calculation of the rate coefficients for the different exit channels using an importance sampling Monte Carlo method.

For completeness, the main points related to the rate coefficient calculation are summarized. The thermal rate coefficient from trajectory calculations is determined from¹⁰

$$k(T_t, T_{rv}, T_e) = \frac{\beta_t}{g(T_e)} \sqrt{\frac{8\beta_t}{\pi\mu}} \int_0^\infty \sigma(E_c; T_{rv}) E_c e^{-\beta_t E_c} dE_c, \quad (2)$$

where $\beta_t = k_B T_t$ and k_B is the Boltzmann constant; T_t , T_{rv} , and T_e are the translational temperature of NO and O, the rovibrational temperature of NO, and the electronic temperature of NO, respectively; $g(T_e)$ is the electronic degeneracy

factor;^{8,11} μ is the reduced mass of NO1 and O₂; and $\sigma(E_c; T_{rv})$ is the integral cross section as a function of the collision energy, E_c and T_{rv} . Throughout the work, it was assumed that $T_t = T_{rv} = T_e$. In other words, the various degrees of freedom in the reactants are in thermal equilibrium. If no subscript is shown for T then it corresponds to the common temperature. In a similar manner, the reaction cross section $\sigma(E_c; T_{rv})$ for a given collision energy E_c is

$$\sigma(E_c; T_{rv}) = \frac{\sum_{v=0}^{v_{\max}} \sum_{j=0}^{j_{\max}(v)} (2j+1) e^{-\beta_{rv} E_{vj}} \sigma_{vj}(E_c; v, j)}{\sum_{v=0}^{v_{\max}} \sum_{j=0}^{j_{\max}(v)} (2j+1) e^{-\beta_{rv} E_{vj}}}, \quad (3)$$

where $\sigma_{vj}(E_c)$ is the (v, j) -state dependent cross section at collision energy E_c . The energy E_{vj} of a rovibrational state (v, j) is calculated according to a Morse oscillator model for the NO molecule.¹² The cross section as an integral of the opacity function $P_{vj}(b; E_c)$ for given E_c and rovibrational state (v, j) is

$$\sigma_{vj}(E_c) = \int_0^\infty P_{vj}(b; E_c) 2\pi b db. \quad (4)$$

The integral in Eq. (2) can be calculated by using an importance sampling Monte Carlo scheme.¹³ For this, the vibrational and rotational quantum numbers, v and j , and the collision energy (E_c) are sampled from the Boltzmann-weighted probability distribution function

$$p_{vj}(T_{rv}) = \frac{(2j+1) e^{-\beta_{rv} E_{vj}}}{\sum_{v'=0}^{v_{\max}} \sum_{j'=0}^{j_{\max}(v')} (2j'+1) e^{-\beta_{rv} E_{v'j'}}}, \quad (5)$$

and

$$\rho(E_c) dE_c = \beta_t^2 E_c e^{-\beta_t E_c} dE_c, \quad (6)$$

respectively.

To determine the upper limit (b_{\max}) of the relevant sampling interval for the impact parameter, b , preliminary tests were carried out at low temperatures (100 and 200 K). As NO₂ was not formed for $b \geq 26 a_0$, the impact parameter was

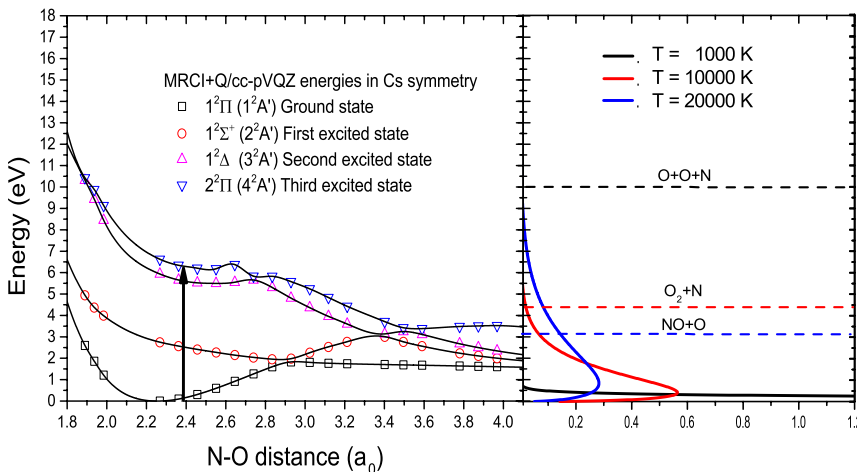


FIG. 2. MRCI+Q/cc-pVQZ energies (symbols) for the O-NO coordinate with the other N-O distance fixed at $r_{NO} = 2.25 a_0$ for linear NO₂ arrangement. The solid lines are RKHS interpolants for each electronic state. The energy gap between the ground and third electronic state has been indicated by a vertical arrow. The panel on the right hand side reports the probability distribution function $P(E)$ for the total energy E . The energies to reach the NO+O, O₂+N and O+O+N asymptotes, taking the global minimum as reference, are indicated by black, red and blue dashed lines, respectively.

uniformly sampled between 0 and $b_{\max} = 26 a_0$. Depending on the temperature, the opacity functions decay to zero by $12 a_0$. Thus, the upper limit is very conservative and ensures convergence of the results with respect to b . However, large impact parameters are required for low-energy collisions.⁷

After evaluating the integral in Eq. (2) over v , j , and E_c , the resulting expression for $k(T)$ is

$$k(T) = \sqrt{\frac{8}{\pi\mu\beta}} \frac{2\pi b_{\max}}{g(T)N_{\text{tot}}} \sum_{i=1}^{N_{\text{reac}}} b_i, \quad (7)$$

where N_{reac} and N_{tot} are the number of reactive and the total number of trajectories, respectively, and b_i is the impact parameter of reactive trajectory i . The convergence of the integral in Eq. (2) was monitored by the decrease of the Monte Carlo error. Choosing eigenenergies from a Morse-oscillator for the NO molecule was done for convenience. To quantify the expected difference in using a kernel-interpolated 1-dimensional potential for the NO oscillator, the bound states from the Morse-fit and the RKHS were determined up to $v = 6$ (corresponding to $\approx 12\,000 \text{ cm}^{-1}$). The correlation between the two sets of eigenenergies is better than 0.999 with a slope of 1.0003. Hence, over the relevant energy range, the initial conditions from a Morse-oscillator model are expected to closely reflect those from using the more accurate kernel-interpolated potential.

The rate coefficients for the reverse ($k_{-}(T)$) and forward reaction ($k_{+}(T)$) derived directly from trajectory calculations in the present work are reported in Figure 3 for temperatures between 300 and 20 000 K. An inset with results for the range from 1000 to 5000 K has also been included. The curve from this work represents a fit to a modified Arrhenius equation (see Eq. (8)).¹⁴ A total of 10 000 trajectories was run for the NO + O reaction whereas only 5000 were necessary for the reverse reaction to obtain a rate coefficient with a relative error of better than 10%. It is found that a directly measured data point at 3000 K (green star) agrees very favorably with the atomistic simulations (magenta) for $k_{+}(T)$,⁷

$$k(T) = AT^n e^{-E_a/T}, \quad (8)$$

where A is the pre-exponential factor and E_a is the activation energy. The parameters resulting from the fit are $A = 9.35 \times 10^8 \text{ cm}^3 \text{ s}^{-1} \text{ mol}^{-1} \text{ K}^{-n}$, $E_a = 1.88 \times 10^4 \text{ kcal/mol}$, and $n = 0.93$.

Forward rate coefficients ($k_{+}(T)$) have been reported in previous works most of which were based on computation. Valli *et al.* reported $k_{+}(T)$ from quasi-classical trajectory calculations using the ground state PES of the NO₂ molecule for temperatures ranging from 300 to 500 K.¹⁵ These data have been extended to higher temperatures by means of a fit to Eq. (8). The resulting parameters are $A = 1.65 \times 10^{13} \text{ cm}^3 \text{ s}^{-1} \text{ mol}^{-1} \text{ K}^{-n}$, $E_a = 2.13 \times 10^4 \text{ kcal/mol}$, and $n = 0$. In the review of reactions relevant to combustion chemistry by Baulch *et al.*, $k_{+}(T)$ for temperatures ranging from 1000 to 5000 K are reported and fit to Eq. (8) with parameters $A = 6.87 \times 10^8 \text{ cm}^3 \text{ s}^{-1} \text{ mol}^{-1} \text{ K}^{-n}$, $E_a = 1.9 \times 10^4 \text{ kcal/mol}$, and $n = 1.13$.¹⁶

Bose *et al.* reported rate coefficients $k_{-}(T)$ for the reverse reaction based on QCT on the ²A' and ⁴A' PESs for temperatures ranging from 1000 to 14 000 K.¹⁷ In order to obtain the forward reaction rate coefficients using Eq. (1), these data were combined with CEA data^{5,6} for the equilibrium rates $K(T)$ (available from 300–20 000 K). These results were extended over the whole temperature range from 300 to 20 000 K by fitting Eq. (8) which yielded the following parameters: $A = 2.49 \times 10^9 \text{ cm}^3 \text{ s}^{-1} \text{ mol}^{-1} \text{ K}^{-n}$, $E_a = 0.4 \times 10^4 \text{ kcal/mol}$, and $n = 1.18$.

At lower temperatures (below 1000 K), experimental data are available for k_{+} which compares within a factor of 3 with the computed values. At sufficiently low temperatures, quantum effects (zero point energy and tunneling) will become important. A recent study of the proton transfer reaction in malonaldehyde has established that zero point effects can play an important role whereas tunneling probably only becomes important at the lowest temperatures.¹⁸ However, this temperature range is not of primary importance for the present work.

The equilibrium rates from the present work obtained directly from the trajectory calculations are compared to the equilibrium constants calculated from the CEA database^{5,6,20} in Figure 4 for temperatures between 5000 and 20 000 K. For temperatures below 6000 K, the CEA functions are fit to available experimental data whereas above 6000 K, the CEA results have been obtained from usual statistical thermodynamic expressions for equilibrium rates, based on spectroscopic constants of the atoms and molecules involved. The results in Figure 4 show that CEA equilibrium constants are somewhat underestimated for temperatures below 10 000 K and agree almost quantitatively for higher temperatures.

In conclusion, the equilibrium rate coefficient for the $\text{O}(^3\text{P}) + \text{NO}(^2\Pi) \leftrightarrow \text{O}_2(X^3\Sigma_g^-) + \text{N}(^4\text{S})$ reaction was calculated directly from molecular dynamics simulations on accurate PESs fitted to high-level electronic structure calculations. The $K(T)$ thus obtained compare favorably with experimental measurements from CEA over a wide temperature range extending up to 20 000 K.^{5,6,20} The influence of higher

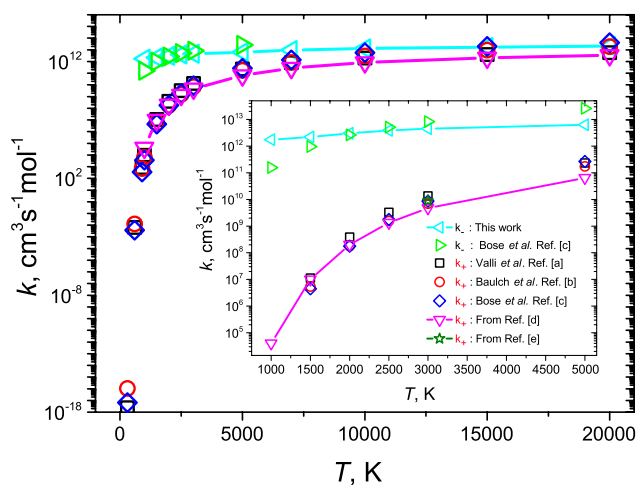


FIG. 3. Rate coefficients $k_{-}(T)$ (blue open triangles) and $k_{+}(T)$ (red open triangles) for temperatures between 300 and 20 000 K. An inset with results for the range from 1000 to 5000 K has been included. In the legend [a] = Ref. 15, [b] = Ref. 16, [c] = Ref. 17, [d] = Ref. 7, and [e] = Ref. 19.

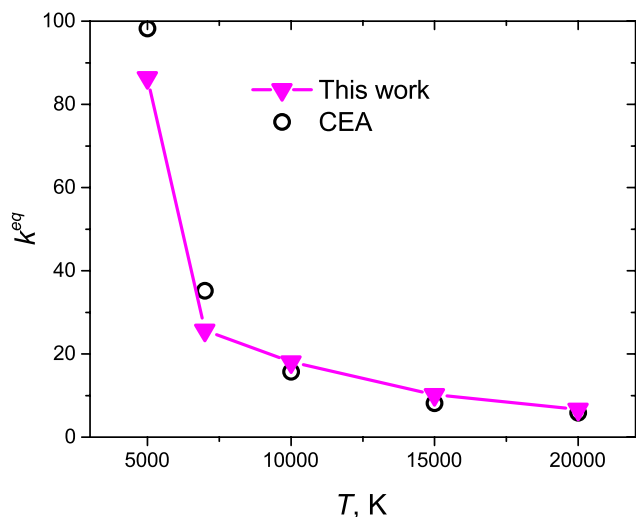


FIG. 4. Equilibrium rate coefficients $K(T)$ for temperatures between 5000 and 20 000 K. Results from CEA are also included for comparison.^{5,6}

electronic states for higher temperature is minor. The forward rate coefficients from this work have been validated against theoretical results from previous works^{15–17} and the present ansatz provides a generic computational framework for obtaining such data from computation.

Part of this work was supported by the United State Department of the Air Force which is gratefully acknowledged (J.C.C.P.) Support by the Swiss National Science Foundation through Grant Nos. 200021-117810, the NCCR MUST (M.M.), and the University of Basel is also acknowledged.

- ¹K. Yoshino, J. Esmond, and W. Parkinson, *Chem. Phys.* **221**, 169–174 (1997).
- ²W. Schneider, G. Moortgat, G. Tyndall, and J. Burrows, *J. Photochem. Photobiol. A* **40**, 195–217 (1987).
- ³T. Corcoran, E. Beiting, and M. Mitchell, *J. Mol. Spectrosc.* **154**, 119–128 (1992).
- ⁴T. Schwartzenruber, L. Scalabrin, and I. Boyd, *J. Spacecr. Rockets* **45**, 1196–1206 (2008).
- ⁵S. Gordon and B. J. McBride, *Computer Program for Calculation of Complex Chemical Equilibrium Compositions and Applications* (NASA Reference Publication, 1996), p. 1311.
- ⁶B. McBride, M. Zehe, and S. Gordon, NASA Report TP-2002-211556, 2002.
- ⁷J. Castro-Palacio, T. Nagy, R. Bemish, and M. Meuwly, *J. Chem. Phys.* **141**, 164319 (2014).
- ⁸L. Harding, H. Stark, J. Troe, and V. Ushakov, *Phys. Chem. Chem. Phys.* **1**, 63–72 (1999).
- ⁹T. S. Ho and H. Rabitz, *J. Chem. Phys.* **104**, 2584–2597 (1996).
- ¹⁰R. D. Levine, *Molecular Reaction Dynamics* (Cambridge University Press, Cambridge, 2005).
- ¹¹J. Duff and R. D. Sharma, *J. Chem. Soc., Faraday Trans.* **93**, 2645–2649 (1997).
- ¹²R. N. Porter, L. M. Raff, and W. H. Miller, *J. Chem. Phys.* **63**, 2214–2218 (1975).
- ¹³D. Frenkel and B. Smit, *Understanding Molecular Simulation. From Algorithms to Applications*, 2nd ed. (Academic Press, London, 2001).
- ¹⁴A. D. McNaught and A. Wilkinson, *IUPAC. Compendium of Chemical Terminology*, The Gold Book 2nd ed. (Blackwell Scientific Publications, Oxford, 1997).
- ¹⁵G. Valli, R. Orru, E. Clementi, A. Lagana, and S. Crocchianti, *J. Chem. Phys.* **102**, 2825–2832 (1995).
- ¹⁶D. Baulch, C. Cobos, R. Cox, G. Frank, P. Hayman, T. Just, J. Kerr, T. Murrells, M. Pilling, J. Troe, R. Walker, and J. Warnatz, *J. Phys. Chem. Ref. Data* **23**, 847–1033 (1994).
- ¹⁷D. Bose and G. V. Candler, *J. Chem. Phys.* **107**, 6136–6145 (1997).
- ¹⁸J. Huang, M. Buchowiecki, T. Nagy, J. Vanicek, and M. Meuwly, *Phys. Chem. Chem. Phys.* **16**, 204–211 (2014).
- ¹⁹T. Clark, S. H. Garnett, and G. B. Kistiak, *J. Chem. Phys.* **51**, 2885–2891 (1969).
- ²⁰L. Gurvich, I. Veyts, and C. Alcock, *Thermodynamic Properties of Individual Substances*, 4th ed. (Hemisphere Publishing Corp., Washington, DC, 1989).